eFigures, eTables, eText, and eReferences

Table of Contents

eFigures

eFigure 1. An overview of our approach to identifying prognostic germline variants. Whole exome sequenced normal (WXS Normal), whole exome sequenced tumor (WXS Tumor), and RNA sequenced tumor (RNA Tumor) samples from 10,582 cancer patients from The Cancer Genome Atlas (TCGA) were variant called. The three variant call sets were merged to create a single Combined variant call set that was used in the rest of the analysis. The variants were filtered to include only common variants that were concordant between the three sequencing datasets. We tested variants for an association with patient outcomes while controlling for clinical covariates using Cox regression models.

eFigure 1

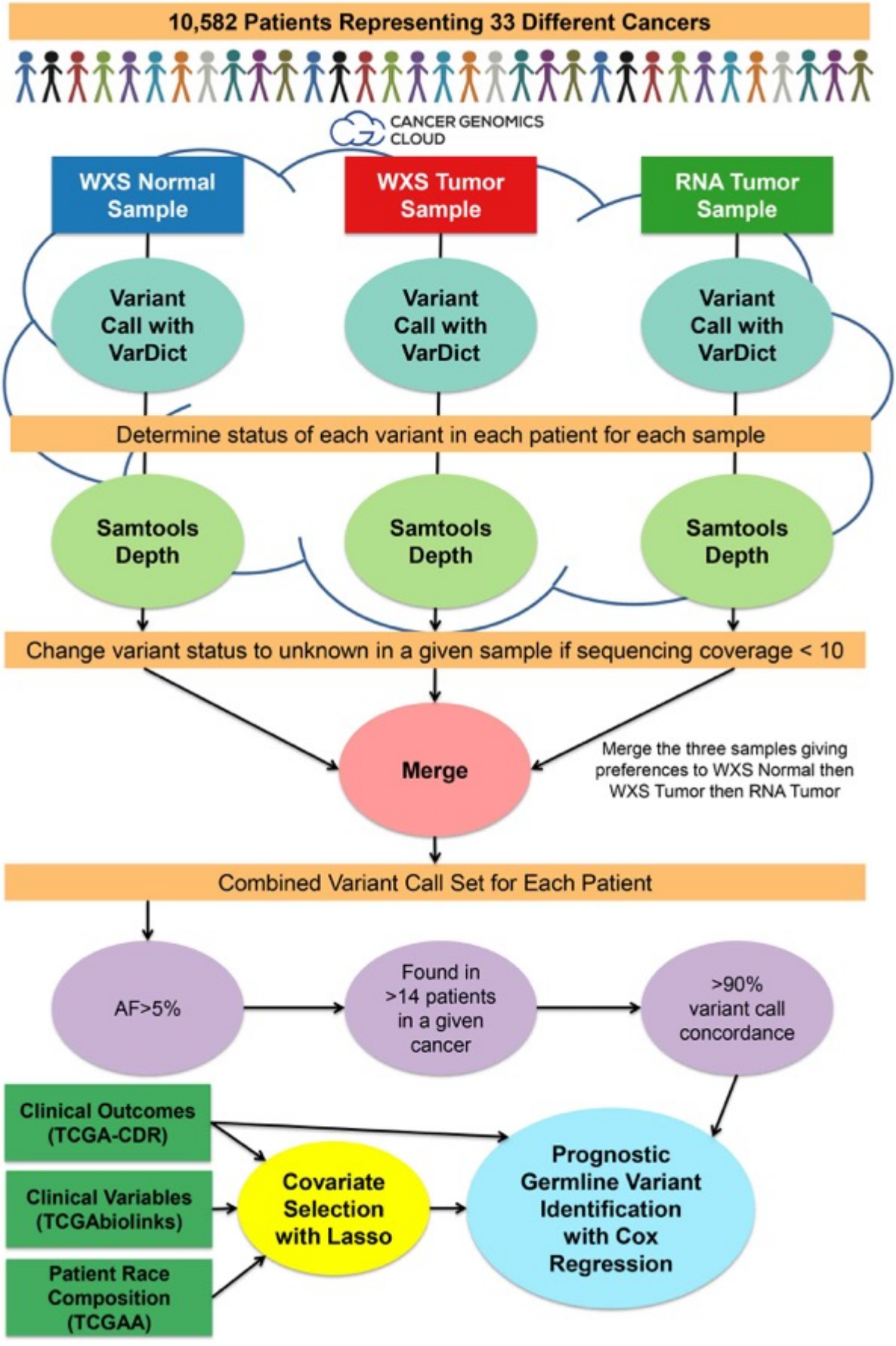
10,582 Patients Representing 33 Different Cancers
CANCER GENOMICS CLOUD
WXS Normal Sample
WXS Tumor Sample
RNA Tumor Sample
Variant Call with VarDict
Variant Call with VarDict
Variant Call with VarDict
Determine status of each variant in each patient for each sample
Samtools Depth
Samtools Depth
Samtools Depth
Change variant status to unknown in a given sample if sequencing coverage < 10
Merge
Merge the three samples giving preferences to WXS Normal then WXS Tumor then RNA Tumor
Combined Variant Call Set for Each Patient
AF>5%
Found in >14 patients in a given cancer
>90% variant call concordance
Clinical Outcomes (TCGA-CDR)
Clinical Variables (TCGAbiolinks)
Patient Race Composition (TCGAA)
Covariate Selection with Lasso
Prognostic Germline Variant Identification with Cox Regression

eFigure 2. An overview of the total number of germline variants called and removed by the various filters included in this analysis. 519,319 germline variants were analyzed in this study.

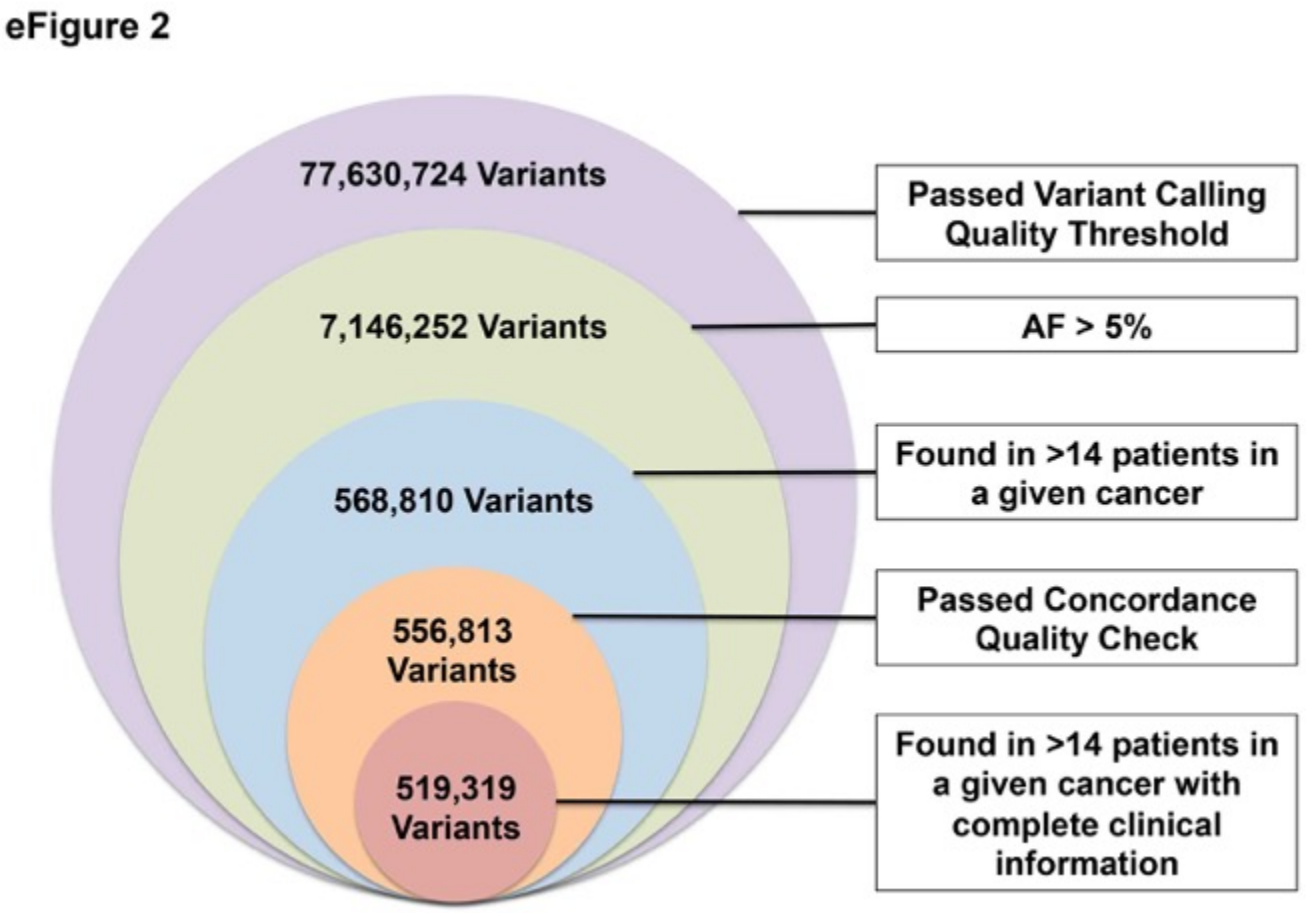

eFigure 3. Somatic mutations did not compromise the integrity of this study.

A. Most variants called from the tumor samples were germline variants. We plotted the percentage of variants called in the whole exome sequenced tumor (WXST) sample that were somatic mutations (SM) across all cancers.

B. Few germline variants (GV) cause the same base change as a somatic mutation (SM) across all the cancers after filtering.

C. Few germline variants (GV) included in this analysis overlap in genomic position with a somatic mutation (SM).

eFigure 3

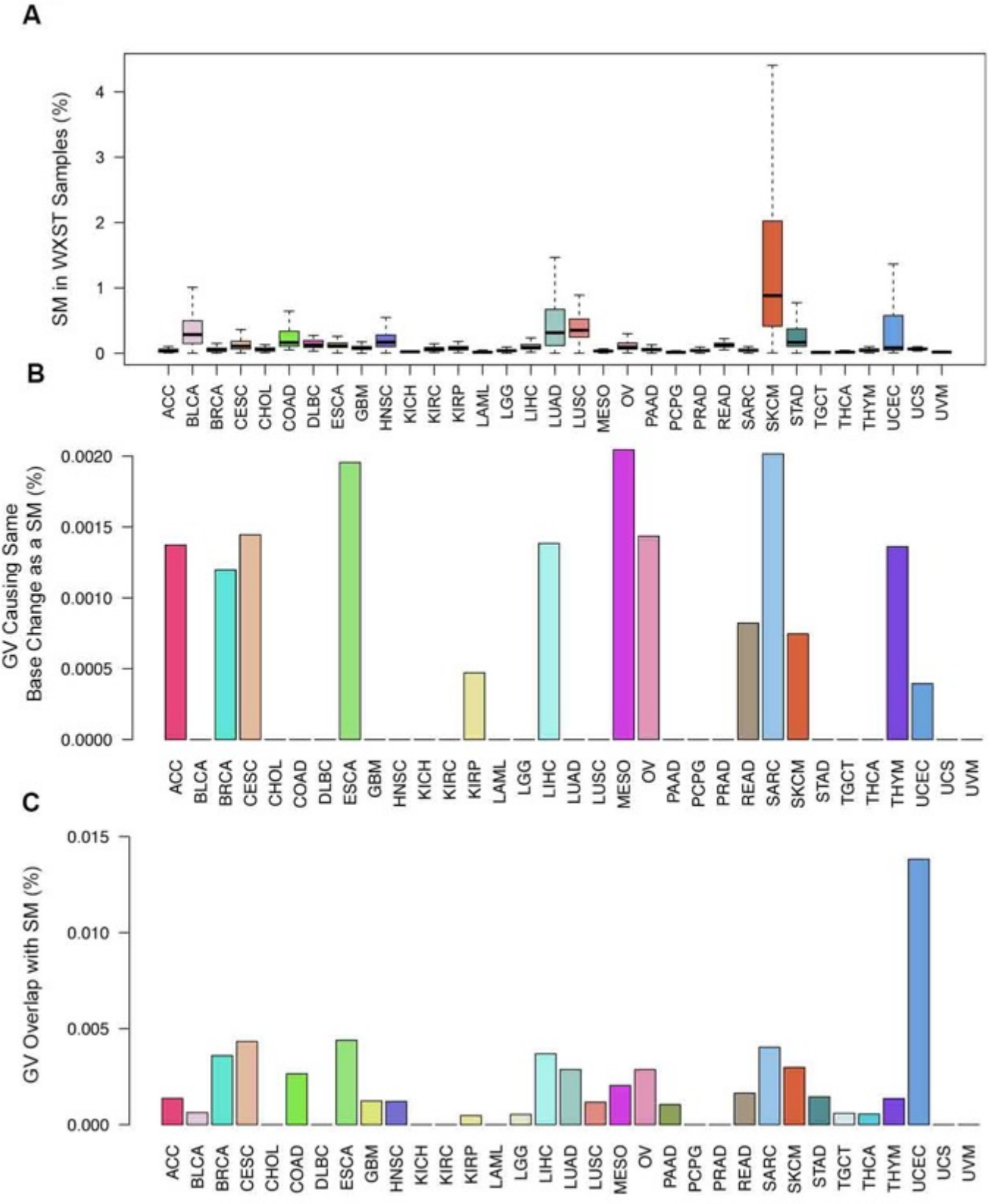
A
SM in WXST Samples (%)
0
1
2
3
4
ACC
BLCA
BRCA
CESC
CHOL
COAD
DLBC
ESCA
GBM
HNSC
KICH
KIRC
KIRP
LAML
LGG
LIHC
LUAD
LUSC
MESO
OV
PAAD
PCPG
PRAD
READ
SARC
SKCM
STAD
TGCT
THCA
THYM
UCEC
UCS
UVM
B
GV Causing Same
Base Change as a SM (%)
0.0000
0.0005
0.0010
0.0015
0.0020
C
GV Overlap with SM (%)
0.000
0.005
0.010
0.015

eFigure 4. RNA editing did not affect the integrity of this analysis.

A. Few germline variants (GV) included in this study overlap with a known RNA editing site in genomic position.

B. Most germline variants are called in the whole exome sequenced samples (WXS). A relatively small number of germline variants were called solely from the RNA sequenced tumor (RNAT) sample.

C. The variant calls from the whole exome sequenced normal (WXSN), whole exome sequenced tumor (WXST), RNA sequenced tumor (RNAT), and Combined (the three variant call sets merged together) are highly concordant with each other. We calculated the allele frequency of each variant in each variant call set and calculated the Spearman correlation coefficient between all pairs.

eFigure 4

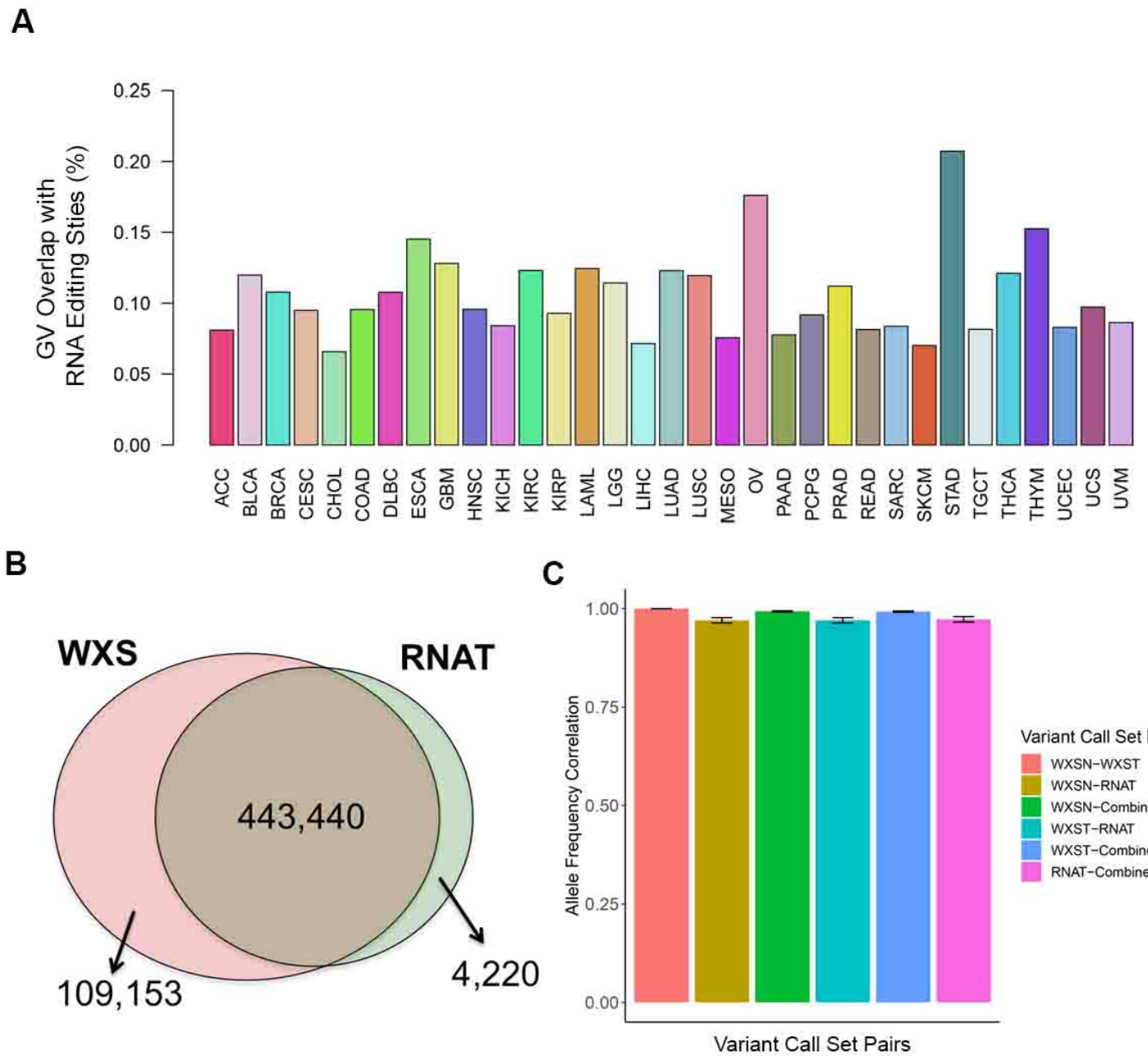
A
GV Overlap with RNA Editing Sties (%)
0.25
0.20
0.15
0.10
0.05
0.00
ACC
BLCA
BRCA
CESC
CHOL
COAD
DLBC
ESCA
GBM
HNSC
KICH
KIRC
KIRP
LAML
LGG
LIHC
LUAD
LUSC
MESO
OV
PAAD
PCPG
PRAD
READ
SARC
SKCM
STAD
TGCT
THCA
THYM
UCEC
UCS
UVM
B
WXS
RNAT
443,440
109,153
4,220
C
Allele Frequency Correlation
1.00
0.75
0.50
0.25
0.00
Variant Call Set Pairs
Variant Call Set P
WXSN−WXST
WXSN−RNAT
WXSN−Combined
WXST−RNAT
WXST−Combined
RNAT−Combined

eFigure 5. Power analysis results depicting the percentage of germline variants with greater than 80% power to detect an association between variant status and patient outcome in individual cancers assuming varying effect sizes. To estimate our statistical power, we randomly sampled 10,000 germline variants in each cancer in each iteration and calculated our statistical power to detect an association between each germline variant and patient outcome.

eFigure 5

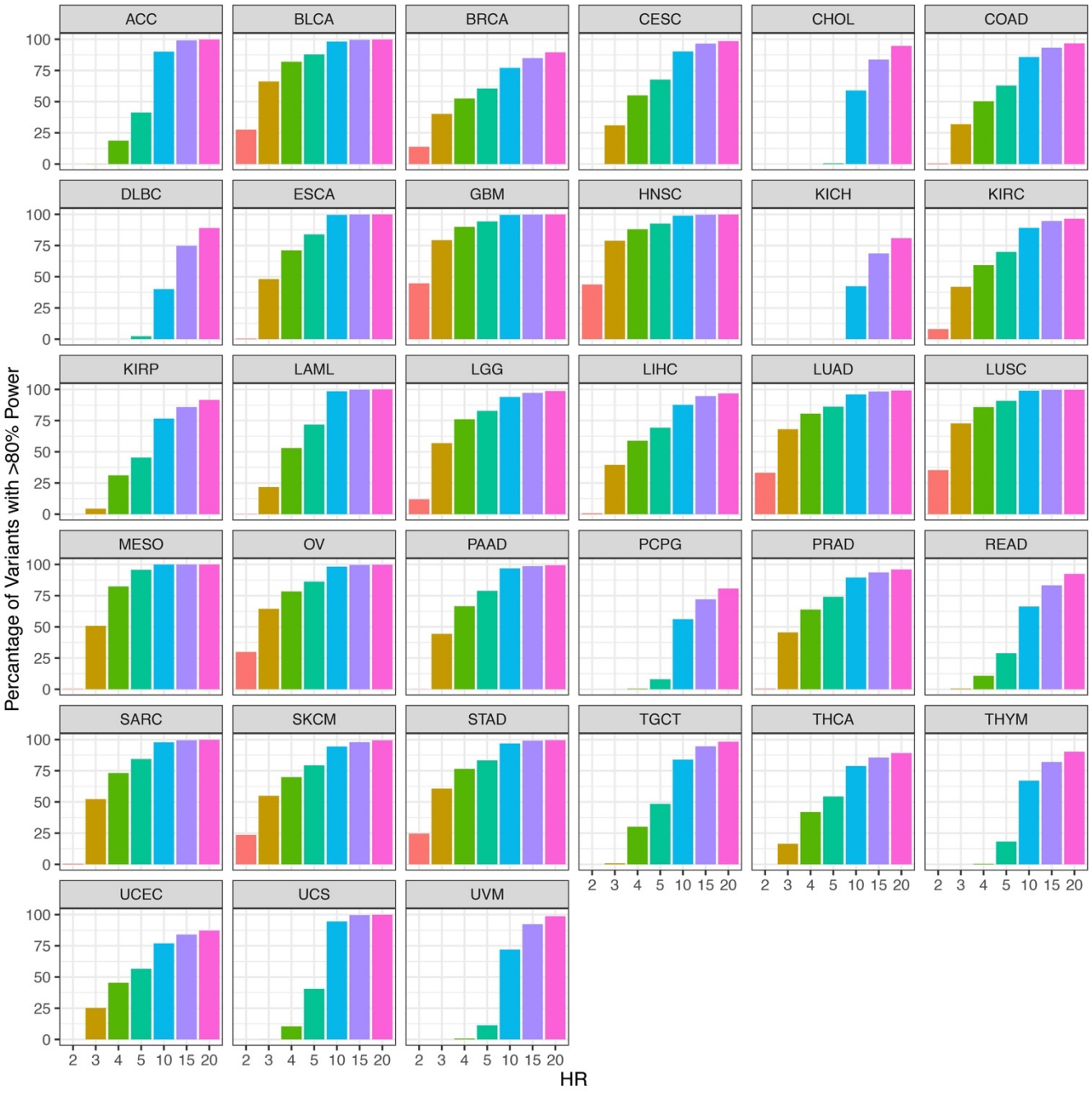
ACC
BLCA
BRCA
CESC
CHOL
COAD
DLBC
ESCA
GBM
HNSC
KICH
KIRC
KIRP
LAML
LGG
LIHC
LUAD
LUSC
MESO
OV
PAAD
PCPG
PRAD
READ
SARC
SKCM
STAD
TGCT
THCA
THYM
UCEC
UCS
UVM
Percantage of Variants with >80% Power
0
25
50
75
100
2 3 4 5 10 15 20
HR

eFigure 6. Selected Kaplan-Meier curves from the variants identified in Analysis 3 in which related cancers were grouped together prior to testing for association with survival.

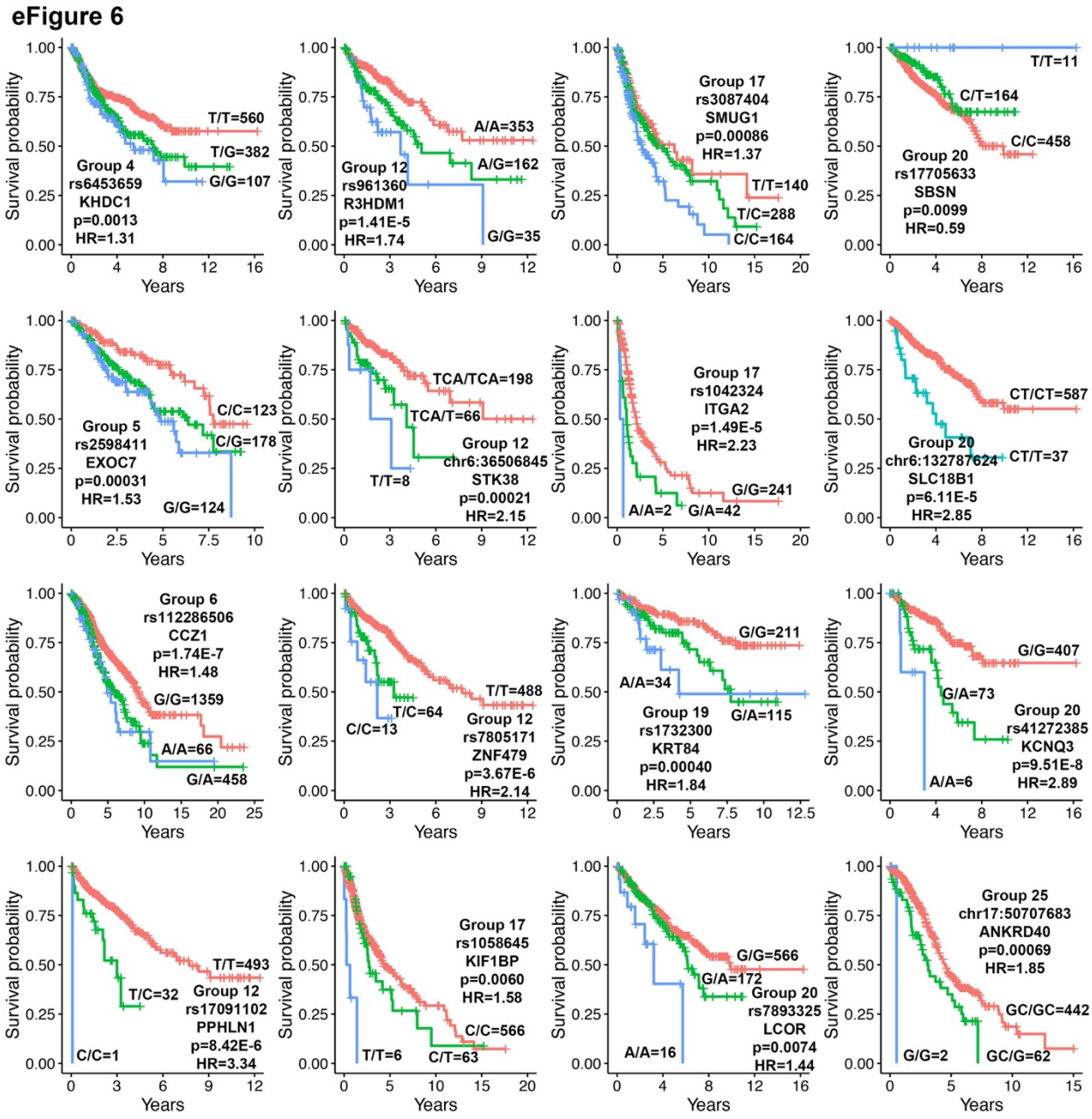

eFigure 7. Schematic representations of how rs1558526, rs6174114, and rs35602605 may perturb well characterize protein domains.

A. rs1558526 is associated with favorable patient outcome in OV in the secreted protease inhibitor *A2ML1*. Wild type *A2ML1* inhibits proteases by forming a covalent bond following cleavage of its central bait domain (left). C970 facilitates the formation of this covalent bond. rs1558526 causes a C970Y amino acid change that likely disrupts *A2ML1*'s ability to inhibit proteases (right).

B. rs6174114 in *CRYBG1/AIM1* is associated with poor patient outcome in PAAD. The binding of *CRYBG1* to actin requires its 12 βγ crystallin motifs and results in suppression of pro-invasion phenotypes. rs6174114 causes a L1235P amino acid change in the fifth βγ crystallin motifs that may disrupt the packing of the beta sheets and perturb *CRYBG1*'s function, likely leading to increased tumor invasiveness and poor patient outcome.

C. rs35602605 in *EIF2AK4/GCN2* is associated with poor prognosis in THCA. *EIF2AK4* decreases translation of some proteins and increases translation of others (such as *CDKN1A*) under conditions of stress by binding uncharged tRNAs through its histidyl-tRNA-synthetase domain. rs35602605 results in a G1306S amino acid change in the histidyl-tRNA synthetase-like domain. This variant may disrupt the function of *EIF2AK4* resulting in poor patient outcome.

eFigure 7

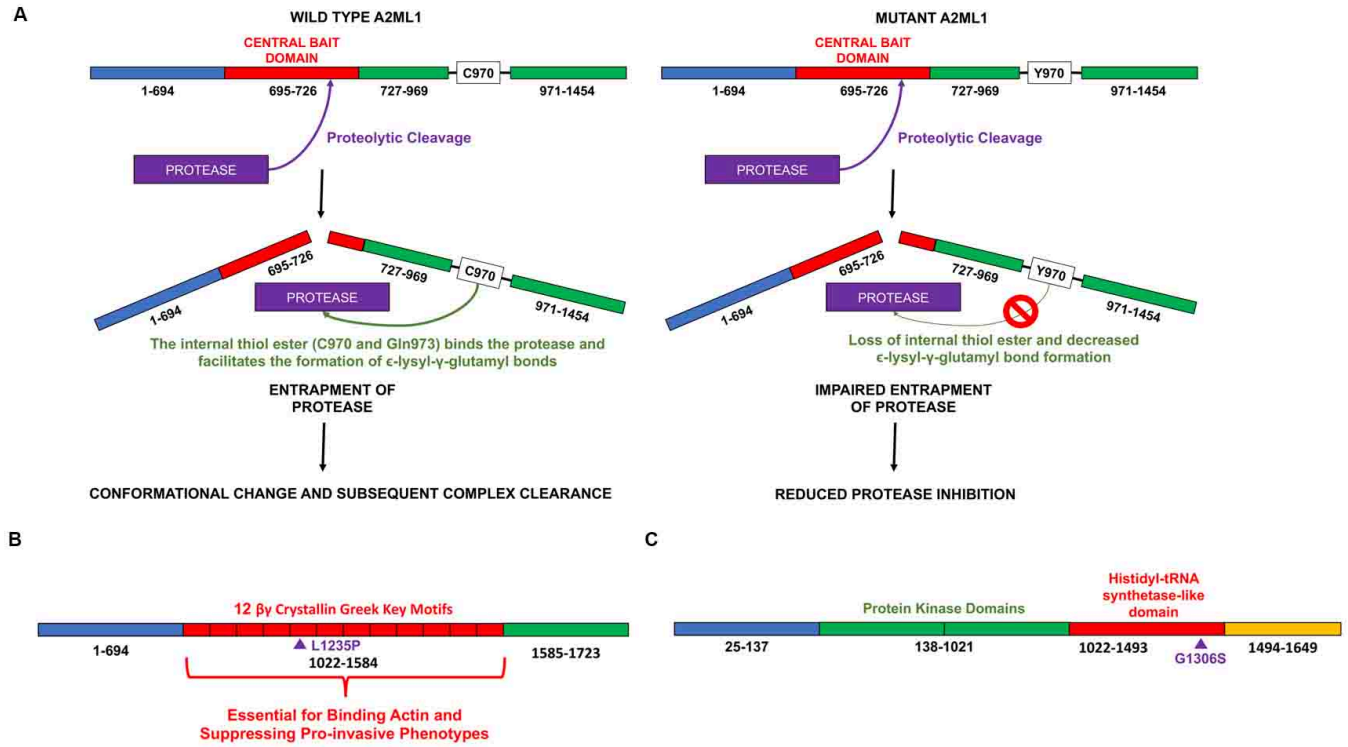

eTables

eTable 1. Clinical information about the patients included in this study and the covariates that we controlled for in our Cox regression models that were selected using Lasso-regularization.

Abbreviation	Cancer	Sample Size	Endpoint	Covariates
ACC	Adrenocortical carcinoma	91	OS	Age, Gender, Race, Stage
BLCA	Bladder Urothelial Carcinoma	410	OS	Age, Height, Stage
BRCA	Breast invasive carcinoma	1079	OS	Age, Estrogen Receptor Status
CESC	Cervical squamous cell carcinoma and endocervical adenocarcinoma	294	OS	Age, Histological Type, Race, Stage
CHOL	Cholangiocarcinoma	45	OS	Albumin Level, Race
COAD	Colon adenocarcinoma	441	OS	Age, Anatomic Position, Race, Stage
DLBC	Lymphoid Neoplasm Diffuse Large B-cell Lymphoma	47	PFI	None
ESCA	Esophageal carcinoma	184	PFI	Histological Type, Anatomic Location, Weight
GBM	Glioblastoma multiforme	390	OS	Age, Chr 19/20 co-gain, Gender, IDH Mutation Status
HNSC	Head and Neck squamous cell carcinoma	523	OS	Age, Anatomic Location, Grade, Race, Stage
KICH	Kidney Chromophobe	65	PFI	Age, Stage
KIRC	Kidney renal clear cell carcinoma	530	OS	Age, Gender, Grade, Hemoglobin Level, Platelet Count, Race, Stage, White Blood Cell Count
KIRP	Kidney renal papillary cell carcinoma	286	OS	Stage
LAML	Acute Myeloid Leukemia	131	OS	Age, Cytogenetics Risk, Morphology
LGG	Brain Lower Grade Glioma	510	OS	1p/19q co-deletion status, Age, Chr 7 gain/Chr 10 Loss Status, Grade, IDH Mutation Status
LIHC	Liver hepatocellular carcinoma	369	OS	Age, Alcohol Consumption History, Fetoprotein Value, Grade, Platelet Count, Race, Stage
LUAD	Lung adenocarcinoma	506	OS	Stage
LUSC	Lung squamous cell carcinoma	497	OS	Age, Anatomic Location, Race
MESO	Mesothelioma	85	OS	Age, Histological Type
OV	Ovarian serous cystadenocarcinoma	523	OS	Age, Anatomic Location, Grade, Race, Stage

PAAD	Pancreatic adenocarcinoma	184	OS	Age, Anatomic Location, Gender, Grade, Race, Smoking History, Stage
PCPG	Pheochromocytoma and Paraganglioma	177	PFI	None
PRAD	Prostate adenocarcinoma	498	PFI	Anatomic Location, Gleason Grade, Race
READ	Rectum adenocarcinoma	163	PFI	Age, Gender, Race, Stage
SARC	Sarcoma	260	OS	Age, Pathology Margin Status, Postoperative Treatment, Residual Tumor
SKCM	Skin Cutaneous Melanoma	437	OS	Age, Breslow Depth Value, Race, Stage
STAD	Stomach adenocarcinoma	416	OS	Age, Anatomic Location, Grade, Stage, Race
TGCT	Testicular Germ Cell Tumors	134	PFI	Anatomic Location, History of Undescended Testis, Race, Stage
THCA	Thyroid carcinoma	505	PFI	Histological Type, Stage
THYM	Thymoma	122	PFI	None
UCEC	Uterine Corpus Endometrial Carcinoma	544	OS	Age, Grade, Height, Histological Type, Menopausal Status, Race, Stage, Total Pelvic Lymph Node Ratio, Total Pelvic Lymph Nodes Positive, Weight
UCS	Uterine Carcinosarcoma	56	OS	Hypertension, Residual Tumor, Total Pelvic Lymph Node Ratio, Tumor Invasion on Primary Pathology
UVM	Uveal Melanoma	80	OS	Age, Morphology, Tumor Diameter, Year of Diagnosis

eTable 3. Justification for the groups presented in **Figure 1D**.

Group Number	Group	Group Description
1	ACC, KICH	Clustered by TCGA
2	ACC, PCPG	Adrenal Tumors
3	BLCA, CESC, HNSC, LUSC	Clustered by TCGA
4	BLCA, KICH, KIRC, KIRP	Urinary System
5	BLCA, KIRC, KIRP	Urinary System Without KICH
6	BRCA, OV, UCEC, UCS	Female Reproductive
7	CESC, HNSC, LUSC	Clustered by TCGA
8	CHOL, COAD, ESCA, LIHC, PAAD, READ, STAD	Gastro-intestinal
9	CHOL, LIHC	Bile Production and Storage
10	COAD, ESCA, PAAD, READ, STAD	Digestive System
11	COAD, ESCA, READ, STAD	Gastro-intestinal Tract
12	COAD, READ	Colon
13	COAD, READ, STAD	Lower Gastro-intestinal Tract
14	DLBC, LAML	Blood
15	DLBC, LAML, THYM	Immune System
16	DLBC, PCPG, SARC, THYM, UCS	Clustered by TCGA
17	GBM, LGG	Gliomas
18	GBM, LGG, PCPG	Neuro-endocrine and Gliomas
19	KICH, KIRC, KIRP	Kidney
20	KIRC, KIRP	Kidney without KICH
21	LAML, PRAD, THCA, THYM	Clustered by TCGA
22	LAML, THCA	Clustered by TCGA
23	LUAD, LUSC	Pulmonary without MESO
24	LUAD, LUSC, MESO	Pulmonary
25	OV, UCEC	Pelvic Female Reproductive
26	PAAD, STAD	GI Enzyme Production
27	PRAD, TGCT	Male Reproductive
28	SKCM, UVM	Melanoma
29	UCEC, UCS	Uterus

eText

eText 1. The final set of germline variants included in this analysis are not substantially contaminated by somatic mutations or RNA editing.

Because the final variant call set was created by merging variant calls from WXS Normal, WXS Tumor, and RNA Tumor data, we evaluated our variant calls to ensure that they were not significantly contaminated by somatic mutations or RNA editing.

The total number of somatic mutations in each patient were obtained from the TCGA Research Network.[1] <2% of the total number of variants in a patient prior to any filtering or quality control were somatic mutations (**eFigure 3A**). After filtering, <0.002% of germline variants in a given cancer included in this analysis caused the same base pair change as a somatic mutation (**eFigure 3B**). In fact, <0.02% of germline variants included in this analysis in a given cancer even overlapped in position with a somatic mutation (**eFigure 3C**). Therefore our final variant call set after filtering was not significantly contaminated by somatic mutations.

We next checked whether our variant call set was significantly affected by RNA editing. A set of over 2.5 million known RNA editing sites was identified from the rigorously annotated RNA editing database RADAR[2] and overlapped with the germline variants included in this analysis. <0.25% of germline variants in a given cancer included in this analysis overlapped in position with an RNA editing site (**eFigure 4A**).

79.6% of germline variants were called in both the WXS and RNA samples, 19.6% were called only in the WXS samples, and 0.8% were called only in the RNA samples (**eFigure 4B).** Because a large number of germline variants were called in both the WXS and RNA samples, we were able to evaluate the concordance between the variant calls between the WXS Normal, WXS Tumor, and RNA Tumor samples. The

allele frequency of each variant in each cancer in all four variant call sets (WXS Normal, WXS Tumor, RNA Tumor, and the three variant call sets combined) was calculated and correlated with each other. The allele frequencies in the four variant call sets were very well correlated with each other (**eFigure 4C**), implying that the variant calls between the different samples were highly concordant. Taken together, these results suggest that somatic mutations, RNA editing, and pooling of the variant call sets did not lead to spurious germline variant calls.

Germline variant calling of all of the patients included in TCGA had previously been performed by Huang et al.[3] We found that 93.0% of the variants called by Huang et al. were also found to have the same exact germline variant call in our analysis. For 1.5% of the variant calls there was disagreement between the two tools about whether an individual was heterozygous or homozygous for the alternate allele. 5.53% of the variants were called by GenomeVIP (Huang et al.'s tool) but not VarDict (our tool). <0.07% of the variants were called in VarDict but not GenomeVIP.

The concordance between the two germline variant call sets is quite strong, given the differences between the two studies. Huang et al. had performed variant calling on the WXS Normal samples aligned to hg19 and had performed variant calling using GenomeVIP, which integrates variant calls from Varscan, GATK, and pindel,[4-6] whereas our germline variant calls were generated using VarDict[7] from the WXS Normal, WXS Tumor, and RNA sequenced tumor samples aligned to hg38. Huang et al. implemented a variety of filtering criteria, including requiring an unfiltered allelic depth greater than 5 reads. We required a filtered (we excluded reads with a mapping quality less than 30 and base quality less than 25) read depth of 3 reads per sample and allele

fraction of 5% The level of discordance that we found was expected, given the differences that could result from the usage of different reference genomes during alignment, filtering criteria, and variant calling tools.[7]

eText 2. The results of our power analysis suggest that we can detect associations between germline variants with moderate to high effect sizes and patient outcome.

We evaluated our ability to detect significant associations between germline variants and patient outcome across the thirty-three cancers by calculating statistical power. The power to detect a significant association between a variant and patient outcome is dependent on multiple factors, including sample size, effect size, correlation with other covariates in the survival model, the number of patients with the germline variant, and the number of patients without the germline variant. To get a sense of our likelihood to detect associations across the thirty-three cancers at various effect sizes, we randomly sampled 10,000 germline variants from the pool of testable germline variants and calculated power for each germline variant at hazard ratios of 2, 3, 4, 5, 10, 15, and 20. The results are depicted in **eFigure 5**.

The results suggest that our study design would enable us to detect associations beginning around a hazard ratio of 2. With that said, our power study suggests that for every germline variant that we are able to associate with patient outcome at lower hazard ratios, we will likely fail to detect several others due to having limited statistical power for variants with lower effect sizes, even in the cancers with the largest sample sizes. Future studies with larger sample sizes will be able to detect these associations that our current study will likely miss. Furthermore, it should be noted that even if germline variants fail to be associated with patient outcome, our study is not sufficiently powered to claim that those variants are not in reality associated with outcome. Finally, the results suggest that we are extremely unlike to detect an association with germline variants with low to moderate effect sizes in ACC, CHOL, DLBC, KICH, PCPG, TGCT, THYM, UCS, and UVM.

eText 3. The direction (indicating whether a germline variant is deleterious or protective) and magnitude of the hazard ratio is correlated across cancers in which the germline variant is prognostic.

When looking at the set of variants associated with patient outcome in three or more cancers, we found that the direction of the hazard ratio for a given variant in different cancers in which it was prognostic (HR>1 implying that the variant is deleterious or HR<1 implying that the variant is protective) was much more concordant ($p<2.2E-16$) than we expected based on random chance. Surprisingly, we even found the magnitude of the hazard ratio to be correlated across cancers. We identified the set of variants associated with favorable (HR<1) outcome and deleterious (HR>1) outcome in three or more cancers and found the hazard ratios estimated for a variant in different cancers to be correlated for both the deleterious (HR>1) variants (Spearman rho=0.146, p=5.36E-157) and protective (HR<1) variants (Spearman's rho=0.185, p=2.71E-101). Because previous studies have reported a correlation between effect size of variants identified in GWAS and allele frequency,[8] we considered whether this correlation may be confounded by the allele frequency of these variants. After controlling for allele frequency, we still find a significant partial correlation after analyzing both the deleterious (Spearman rho=0.0667, p=4.024E-34) and protective (Spearman rho=0.0584, p=2.274E-11) variants. These findings reinforce the notion that the prognostic germline variants' effects tend to show some consistency across cancers.

eText 4. The deleterious allele of prognostic germline variants are more likely to be associated with somatic mutations in known cancer driver genes than of non-prognostic germline variants.

A previous study had identified germline variants that were associated with a significant increased incidence of somatic mutations in cancer related genes.[9] We therefore hypothesized that the prognostic variants were associated with an increased incidence of somatic mutations in driver genes in the cancer in which that variant was prognostic. To test this hypothesis, we created 353 germline variant-cancer pairs and determined the number of prognostic variants for which the deleterious allele was associated with an increased incidence of somatic mutations relative to the protective allele. We repeated this analysis for all of the germline variants included in this analysis. We found that 47 of the 353 (13.3%) germline variant-cancer pairs were associated with an increased incidence of mutations in cancer driver genes which is more than expected by random chance (OR=1.89, p=0.0001).

eText 5. A detailed discussion of the twelve germline variants that cause significant amino acid changes.

To demonstrate that the prognostic germline variants identify genes that could be directly or indirectly linked to cancer progression, below we turn to the twelve germline variants in **Figure 5E** that caused substantial amino acid changes. Of these *MAP2K3* has been discussed in the main text.

A2ML1 is a secreted protease inhibitor that inhibits all classes of proteases. When proteases cleave the central bait domain of *A2ML1*, conformational changes cause an internal thiol ester, formed by C970 and Gln973, to become highly reactive. This thiol ester bond binds the protease and facilitates the formation of covalent bonds between *A2ML1* and the protease, resulting in protease entrapment and inhibition.[10] In our analysis, the germline variant rs1558526 was associated with favorable patient outcome in ovarian cancer patients and resulted in a C970Y change in *A2ML1*. Because the very cysteine residue that forms the internal thiol ester is lost, this amino acid change likely disrupts *A2ML1*'s protease inhibition function (**eFigure 7A**). This result suggests that certain extracellular proteases which *A2ML1* may normally inhibit may have anti-tumor effects, for example by degrading angiogenic factors or anti-immune factors.

CRYBG1/AIM1 (absent in melanoma) is a protein that localizes to the cytoskeleton. Loss of *CRYBG1* in prostate cancer cells leads to increased G-actin (relative to F-actin), cell migration, invasion and soft agar colony formation. Binding of *AIM1* to actin requires the six C terminal domains made of 12 βγ crystallin motifs.[11] We found rs6174114 in *CRYBG1* to be associated with poor patient outcome in pancreatic cancer. This variant changes L1235 to P in the fifth domain of *CRYBG1*. Substitution of

proline at this position could disrupt the packing of the beta sheets that make a β or γ motif (**eFigure 7B**), resulting in loss of *CRYBG1* function and therefore increase cell migration, invasion, and soft agar colony formation. This would explain the poor patient outcome associated with this germline variant. Somatic mutation or epigenetic suppression of *CRYBG1* has been seen in melanomas, lymphomas, and prostate carcinoma. Decreased expression of the protein associated with metastasis.[11]

EIF2AK4/GCN2 is a protein kinase that is activated under stress by binding to uncharged tRNAs through its histidyl-tRNA-synthetase domain. This kinase is important for decreasing protein translation and for activating specific translation of genes like *ATF4* and *p21/CDKN1A* under conditions of stress often seen inside tumors like amino acid starvation and glucose starvation. We found the germline variant rs35602605 in *EIF2AK4* to be associated with poor prognosis. This variant causes a G1306S amino acid change in the histidyl-tRNA synthetase-like domain (**eFigure 7C**). This variant may disrupt the ability of the histidyl-tRNA synthetase-like domain to bind uncharged tRNAs and thereby protect the cancer cells from translation of stress-induced genes like *CDKN1A* that restrain tumor proliferation. If true, this would explain the association of this germline variant with poor patient outcome.

The other gene-products identified by prognostic variants in **Figure 5E** also warrant a detailed examination. Two of them could be important for immune response to a tumor. *FCRL6* binds to MHC class II proteins and acts as an immune checkpoint protein that is often upregulated in Tumor infiltrating lymphocytes.[12] It is particularly interesting that *FCRL6* expression of T lymphocytes is decreased five-fold in acute and chronic myeloid leukemias[13] because the rs61823162 variant (which truncates the

protein) is associated with outcome in LAML. *EPHA10* is a non-functional tyrosine kinase receptor for ephrins. The G749E mutation is located in the tyrosine kinase domain, which upregulates PD-L1 protein expression.[14] Three genes are involved in intracellular vesicle transport, membrane fusion and cell migration: *BORCS5* recruits the *ARL8B* GTPase to lysosomes for lysosomal movement and function, *KDELR3* is involved in retaining proteins in the endoplasmic reticulum, and *MYOF* facilitates vesicle fusion. Two are involved in GPCR pathways: *OR10X1 is* an olfactory receptor and *SAG/arrestin1* binds to GPCRs (such as rhodopsin) to terminate signaling. Many olfactory receptors are ectopically expressed in several cancer[15] and their activation decreases cancer cell proliferation and migration and increases apoptosis.[16] The I-76 of *SAG* that is altered by the variation is located in the highly conserved finger loop of motif 2, (E/D)x(I/L)xxxGL, which is extended and buried in the rhodopsin (GPCR)-SAG interface.[17] Finally *ECD/SGT1* associates with many cellular proteins relevant for cancer, *MDM2*, *Rb*, *HSP90*, *SKP1*, and *RUVBL1*, the last in particular using the C-terminal region of *ECD* that is mutated in the prognostic variant.

eReferences

1. Ellrott, K.*, et al.* Scalable Open Science Approach for Mutation Calling of Tumor Exomes Using Multiple Genomic Pipelines. *Cell systems* **6**, 271-281.e277 (2018).
2. Ramaswami, G. & Li, J.B. RADAR: a rigorously annotated database of A-to-I RNA editing. *Nucleic acids research* **42**, D109-113 (2014).
3. Huang, K.L.*, et al.* Pathogenic Germline Variants in 10,389 Adult Cancers. *Cell* **173**, 355-370.e314 (2018).
4. McKenna, A.*, et al.* The Genome Analysis Toolkit: a MapReduce framework for analyzing next-generation DNA sequencing data. *Genome Res* **20**, 1297-1303 (2010).
5. DePristo, M.A.*, et al.* A framework for variation discovery and genotyping using next-generation DNA sequencing data. *Nature genetics* **43**, 491-498 (2011).
6. Van der Auwera, G.A.*, et al.* From FastQ data to high confidence variant calls: the Genome Analysis Toolkit best practices pipeline. *Curr Protoc Bioinformatics* **43**, 11.10.11-33 (2013).
7. Lai, Z.*, et al.* VarDict: a novel and versatile variant caller for next-generation sequencing in cancer research. *Nucleic acids research* **44**, e108 (2016).
8. Park, J.H.*, et al.* Distribution of allele frequencies and effect sizes and their interrelationships for common genetic susceptibility variants. *Proceedings of the National Academy of Sciences of the United States of America* **108**, 18026-18031 (2011).
9. Carter, H.*, et al.* Interaction Landscape of Inherited Polymorphisms with Somatic Events in Cancer. *Cancer discovery* **7**, 410-423 (2017).
10. Galliano, M.F.*, et al.* A novel protease inhibitor of the alpha2-macroglobulin family expressed in the human epidermis. *The Journal of biological chemistry* **281**, 5780-5789 (2006).
11. Haffner, M.C.*, et al.* AIM1 is an actin-binding protein that suppresses cell migration and micrometastatic dissemination. *Nature communications* **8**, 142 (2017).
12. Johnson, D.B.*, et al.* Tumor-specific MHC-II expression drives a unique pattern of resistance to immunotherapy via LAG-3/FCRL6 engagement. *JCI insight* **3**(2018).
13. Kulemzin, S.V.*, et al.* FCRL6 receptor: expression and associated proteins. *Immunology letters* **134**, 174-182 (2011).
14. Yang, W.H.*, et al.* Juxtacrine Signaling Inhibits Antitumor Immunity by Upregulating PD-L1 Expression. *Cancer research* **78**, 3761-3768 (2018).
15. Ranzani, M.*, et al.* Revisiting olfactory receptors as putative drivers of cancer. *Wellcome open research* **2**, 9 (2017).
16. Weber, L.*, et al.* Activation of odorant receptor in colorectal cancer cells leads to inhibition of cell proliferation and apoptosis. *PloS one* **12**, e0172491 (2017).
17. Peterson, Y.K. & Luttrell, L.M. The Diverse Roles of Arrestin Scaffolds in G Protein-Coupled Receptor Signaling. *Pharmacological reviews* **69**, 256-297 (2017).